Turkish Journal of Physics

Volume 38 | Number 3 Article 17

1-1-2014

Device architectures in organic photovoltaics

JAMES T. MCLESKEY JR

Follow this and additional works at: https://journals.tubitak.gov.tr/physics

 Part of the Physics Commons

Recommended Citation

JR, JAMES T. MCLESKEY (2014) "Device architectures in organic photovoltaics," *Turkish Journal of Physics*: Vol. 38: No. 3, Article 17. https://doi.org/10.3906/fiz-1405-18
Available at: https://journals.tubitak.gov.tr/physics/vol38/iss3/17

This Article is brought to you for free and open access by TÜBİTAK Academic Journals. It has been accepted for inclusion in Turkish Journal of Physics by an authorized editor of TÜBİTAK Academic Journals. For more information, please contact academic.publications@tubitak.gov.tr.

Turkish Journal of Physics

http://journals.tubitak.gov.tr/physics/

Invited Review Article

Turk J Phys
(2014) 38: 516 – 525
© TÜBİTAK
doi:10.3906/fiz-1405-18

Device architectures in organic photovoltaics

James T. McLESKEY JR*
Department of Mechanical and Nuclear Engineering Virginia Commonwealth University, Richmond, VA, USA

Received: 29.05.2014 • **Accepted:** 03.06.2014 • **Published Online:** 10.11.2014 • **Printed:** 28.11.2014

Abstract: The various device structures used in organic polymer solar cells are reviewed. The operating principles behind these devices are explained in order to provide the reasoning behind the different structures. The incorporation of nanostructures into both bilayer and bulk heterojunction devices to improve exciton separation, charge transport, and light absorption is discussed. Novel ideas such as electrospun fibers and supramolecules are also covered. Finally, the impact of these structures on overall efficiency is evaluated.

Key words: Polymer photovoltaics, nanostructure

1. Introduction

Although crystalline silicon solar cells (c-Si) dominate the market [1] and the cost of these devices is declining [2], they continue to have limitations. They still have a relatively high energy cost due to the high temperature processing required to make them [3]. Similarly, very high efficiencies (44.7%) have been achieved with concentrating III–V semiconductor tandem cells (http://www.ise.fraunhofer.de), but as one might expect, these are very expensive devices [4].

Over the past 25 years, a number of new materials, primarily organic in nature, have emerged with the potential to provide both lower manufacturing cost (dollars) and lower energy cost cells because they can be fabricated using a variety of solution-based processing techniques [5,6] The organic devices have achieved maximum efficiencies of nearly 11% [7]. Unlike traditional semiconductor solar cells, light absorption in organic semiconductors results in the formation of a Frenkel exciton [8]. In order to separate the excitons into their constituent electrons and holes, these devices rely on an interface between materials with different electron affinities [9]. Therefore, the efficiency of organic solar cells depends heavily not only on the materials used, but also on the device structure. In this paper, the different architectures that have been employed in an attempt to raise the efficiency of organic solar cells are reviewed.

2. Operating principles

As outlined above, organic solar cells operate differently from devices made from silicon and other semiconductor materials. The very first organic solar cells consisted of a single layer of evaporated organic material between 2 metal electrodes (so called homojunctions) [10–15]. Although these devices functioned as photodiodes, their efficiencies were extremely low ($\sim 10^{-5}$%) [11] because they did not have a second material to help separate the excitons.

*Correspondence: jtmcleskey@vcu.edu

The first 2-component organic photovoltaic cells were reported during the 1980s [16]. The devices consisted of thin films of 2 different materials in a bilayer configuration (Figure 1) and showed that at the interface between 2 materials with different electron affinities charge transfer is energetically favorable. This discovery led to the development of bilayer heterojunction polymer solar cells consisting of distinct electron donor and acceptor layers. However, these early devices were still limited in efficiency to approximately 1% [17].

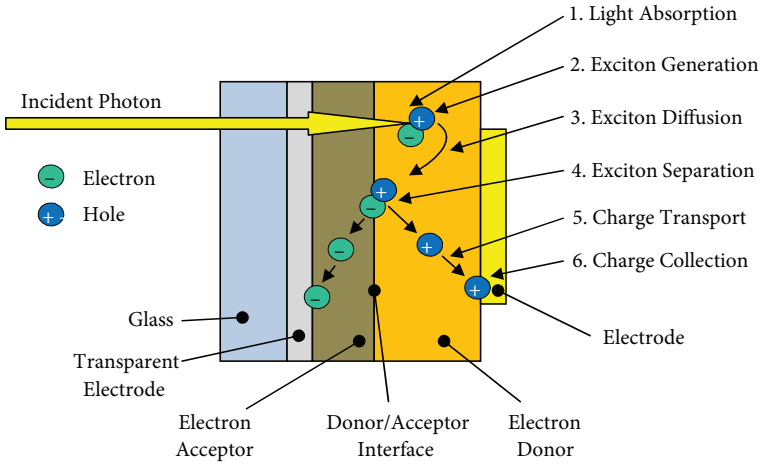

Figure 1. Operational steps in an organic solar cell (bilayer structure shown).

This relatively low efficiency can be understood when one begins to understand the operating principles of organic solar cells. In order to increase the efficiency of organic devices, it is necessary to have some understanding of their operating principles as shown in Figure 1 and outlined below.

2.1. Light absorption and charge generation

In organic solar cells structures, absorption of light typically occurs in the organic material (a dye or polymer). Photons excite electrons from the HOMO level to the LUMO level, resulting in the formation of mobile excited states consisting of tightly bound electron-hole pairs known as Frenkel excitons [8].

2.2. Exciton diffusion and separation

Unlike traditional semiconductors, where the light directly generates free electrons and holes, the electrons and holes in organic materials must be extracted from the excitons. This happens when the excitons diffuse to the interface between 2 materials with different electron affinities [18]. The excitons must reach the interface before recombining. This means that the dimensions of the device structure must be comparable to the exciton diffusion length.

2.3. Charge carrier transport and collection at the electrodes

After separating into distinct electrons and holes at the interface, these charge carriers must be swept (holes and electrons in opposite directions) to the electrodes in order to leave the device. The movement of the carriers depends on the mobility and the continuity of the solar cell materials. If there are any breaks in the material, it will obviously interfere with the movement of the carriers to the electrodes.

3. Polymer cells

3.1. Bilayer heterojunctions

The synthesis of semiconducting organic polymers in the late 1970s [19] led to the development of a variety of new flexible electronic devices, including photovoltaics. Building on the idea of 2-component bilayer solar cells described above, the use of soluble semiconducting polymers to fabricate solar cells began in the early 1990s [20] Sariciftci et al. built a device using poly[2-methoxy-5-(2'-ethyl-hexyloxy)-1,4-phenylene vinylene] [MEH-PPV] and C_{60}. They began by spin-coating the MEH-PPV onto a glass substrate coated with ITO. The fullerenes were then evaporated on top of the MEH-PPV to form a p-n heterojunction. Although these devices had low power conversion efficiencies (only 0.02%) when illuminated with a laser at 514.5 nm, they were the first to use C_{60}, which has become the most commonly used acceptor material.

The low efficiencies in these devices demonstrated the weakness of the bilayer design. The interface between the donor polymer (MEH-PPV) and the accepter material (C_{60}) is relatively flat and therefore the interfacial surface area is quite low. This leads to a narrow-width diffusion region along the interface. Only the light absorbed within the diffusion region will generate an exciton that has an opportunity to separate before recombining and therefore the charge generation in these devices is quite low.

3.2. Bulk heterojunction

The bilayer heterojunction is limited by a small interfacial surface area and therefore, in 1995, 2 groups [21,22] introduced interpenetrating networks of donors and acceptors in what has come to be known as a bulk (or dispersed) heterojunction. In these devices, the electron acceptors (e.g., C_{60}) are blended into the electron donor (e.g., the polymer) to form a composite (Figure 2). This results in a high interfacial area throughout. This means that regardless of where a photon is absorbed in the donor (polymer), the excitons will always be generated within one exciton diffusion length of an interface. This leads to much improved exciton dissociation.

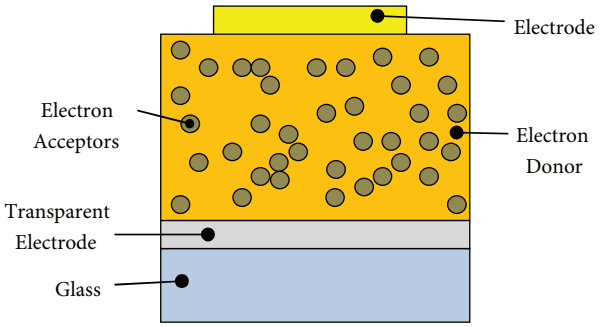

Figure 2. Bulk heterojunction solar cell with high interfacial surface area.

In order to create bulk-heterojunction devices with high interfacial surface areas, Halls et al. [21] blended 2 polymers: MEH-PPV and CN-PPV, while Yu et al. [22] blended MEH-PPV and PCBM (a soluble form of C_{60}). PCBM is now the acceptor of choice in bulk-heterojunction devices. Following on the success of these first bulk heterojunction devices, most devices today are fabricated in this way because of improved charge separation. However, bulk devices still suffer from a problem related to the fact that the electron acceptor material is distributed throughout the layer. Because the acceptor material is discontinuous, conduction takes place by hopping. When the electron hops between acceptor molecules, it often must enter the polymer, where it is subject to recombination.

4. Device structures

Over the past 20 years or so, much effort has been expended to increase efficiency of organic photovoltaics by overcoming the small interfacial area of bilayer heterojunctions and the discontinuous nature of the bulk heterojunction. Some of the strategies that have been incorporated are outlined below.

4.1. Bilayer heterojunctions

In bilayer heterojunctions, the emphasis has been on increasing the interfacial surface area.

4.1.1. Thermal diffusion

Performance of the first class of bilayer devices incorporating C_{60} was limited by the small interfacial area. In order to overcome this problem, Drees et al. introduced "thermally controlled interdiffusion" [23]. They began by depositing 90 nm MEH-PPV via spin coating followed by sublimation of a 100-nm layer of C_{60} on top. The C_{60} and the MEH-PPV were then interfused by placing the device on a hot plate in an inert atmosphere. This caused the C_{60} to diffuse by tens of nanometers into the polymer [24]. The effect is similar to that found in a blended heterojunction in that the C_{60} is now more greatly dispersed throughout the polymer. Excitons generated throughout the polymer now have a smaller distance to travel to reach a material interface and separate. The efficiency (0.30%) [24] under monochromatic illumination showed an order of magnitude increase over that reported by Sariciftci et al. (0.02%) [20].

4.1.2. Nanocrystalline TiO_2

At approximately the same time that polymer solar cells were being developed, the dye sensitized solar cell (DSSC) was also first reported [25]. Using nanocrystalline titanium dioxide (TiO_2) as the electron acceptor. [26], these devices showed remarkably high initial efficiencies ($\sim$7%). Although the DSSC devices required the use of a liquid electrolyte that made commercialization somewhat difficult, the porous nature of the TiO_2 made it a natural choice as the electron acceptor in a polymer solar cell because the surface area is 3 orders of magnitude greater than a comparable flat surface, leading to enhanced exciton separation (Figure 3).

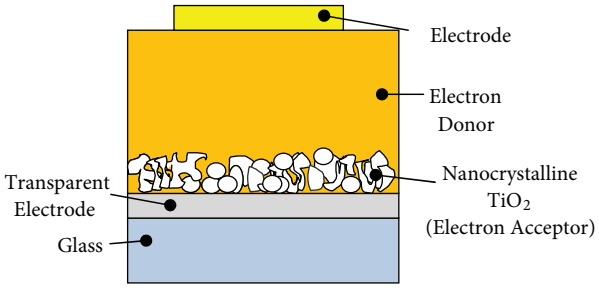

Figure 3. Bilayer organic solar cell incorporating porous nanocrystalline TiO_2 as the electron acceptor leading to higher interfacial surface area.

The first polymer-TiO_2 device was reported in 1998 by Savenije et al [27]. Using MEH-PPV and TiO_2 on an ITO-coated substrate, they achieved a power conversion efficiency of 0.15% under AM1.5 illumination. In spite of the promise shown in these initial devices, the potential advantages of TiO_2, and the use a broad array of different polymers and deposition methods by numerous groups [28–34], the efficiencies of polymer solar cells based on TiO_2 have never exceeded 1%.

4.1.3. Nanorods and nanotubes

Metal oxides can be grown into vertically aligned nanostructures (Figure 4). This has the advantage of allowing the donor–acceptor interfacial area to be optimized while also providing efficient conduction pathways [35]. Building on the use of nanocrystalline TiO_2, Mor et al. fabricated organic–inorganic hybrid solar cells using TiO_2 nanotubes with a poly(3-helylthiophene) P3HT/C_{71} blend and achieved an efficiency of 4.1% [36].

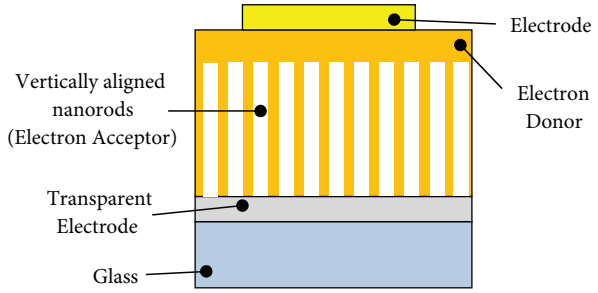

Figure 4. Bilayer organic solar cell incorporating vertically aligned nanostructures.

Other materials have been grown as nanorods as well to form hybrid bilayer heterojunctions. For example, zinc oxide (ZnO) nanorods can be readily grown using wet chemistry techniques and have yielded efficiencies ($\eta \cong 0.20\%$) [37] comparable to those achieved with nanocrysatalline TiO_2 with a maximum power conversion efficiency of 0.76% [38]. In addition to the commonly used hydrothermal methods, other methods of growing ZnO nanorods have been utilized including vapor phase transport deposition [39].

4.2. Bulk heterojunctions

In bulk heterojunctions, the emphasis has been on creating continuous charge carrier pathways.

4.2.1. Nanorods

In bulk heterojunctions, one of the challenges is to create a direct path to the electrodes. Rather than using fullerenes, a number of groups have used nanorod-shaped materials with longer aspect ratios. One of the most successful early efforts was by Alivisatos et al. [40]. Using CdSe nanorods as the electron acceptor, they achieved an overall power conversion efficiency of 1.7%. Within the nanorods, the electron transport occurs by band conduction rather than hopping and, because of this, devices containing longer nanorods showed higher external quantum efficiencies (EQE).

Based on the success of carbon fullerenes and the use of nanorods in bulk heterojunction devices, it was expected that carbon nanotubes would prove to be an effective electron acceptor and the use of carbon nanotubes in polymer solar cells was reported [41,42]. However, the difficulty in separating metallic and semiconducting nanotubes as well as the electrical shorts introduced by the nanotubes proved to be an insurmountable problem and there has been limited work in this area.

In order to gain the benefit of electron transport in nanorod structures while still using C_{60}, Carroll et al. fabricated a device containing PCBM and C_{60}. When this device was annealed, single crystal "nanowhiskers" [6] were formed. This increased the efficiency by approximately 20% over the device, which was not annealed.

4.2.2. Multijunction

The incorporation of nanorods and other structures described above was intended to increase interfacial surface area (to improve exciton separation) and to provide a more direct path to the electrodes (to improve charge transport). Another method for increasing efficiency is to increase light absorption and exciton generation. Multijunction solar cells work by using 2 different layers, each designed to absorb a specific region of the spectrum (Figure 5). This concept was used in thin film devices (e.g., amorphous silicon) [43] for many years before being introduced in polymer solar cells.

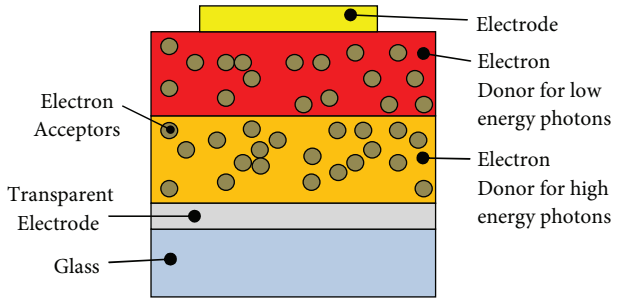

Figure 5. Multijunction solar cell with 2 layers to absorb different parts of the solar spectrum.

Forrest et al. reported the double heterostructure organic solar cell [44,45] in 2000 with an efficiency of 3.6%. These devices included an exciton-blocking layer to prevent electron trapping and mitigate quenching effects caused by cathode deposition damage. The same group later extended the concept to build tandem cells with an efficiency of 5.7% [46]. The highest efficiencies for polymer based solar cells have been achieved in tandem devices [5,7,45,47–56].

4.3. Other structures and techniques

A number of structures and techniques have been investigated in order to increase light absorption, improve exciton separation, and increase charge transport. A few of those methods are outlined below.

4.3.1. Electrospun fibers

Electrospinning uses an electric field to draw polymer fibers from a solution. A hypodermic syringe is filled with an electrically conducting polymer solution. An electric field is then set up between the needle of the syringe and a counter electrode. The polymer solution is drawn out of the syringe by the electric field and a jet moves towards the counter electrode. As the solvent evaporates, solid fibers are formed, which then deposit on the counter electrode.

The fibers produced by electrospinning have diameters on the order of tens of nanometers [57], making them ideally suited to polymer photovoltaics. For example, the small dimensions will help ensure effective exciton separation. In addition, the distances to the electrodes are quite small for improved charged carrier collection. Electrospun fibers have demonstrated a red-shift in absorption and thus offer the possibility of greater charge generation [58]. Finally, the technique is simple and easily scalable, offering the potential for lowers costs.

Sundarrajan et al. were the first to report photovoltaic cells from electropsun conjugated polymer nanofibers [59]. Using a coaxial electrospinning technique, a blend solution of poly(3-hexylthiophene-2,5-diyl) and [6,6]-phenyl C61-butyric acid methyl ester (P3HT/PCBM) in chloroform/toluene was used for the core,

and because the conjugated polymers do not tend to electrospin very well (i.e. they do not form fibers), polyvinylpyrrolidone (PVP) in chloroform/ethanol was used for the shell. A structure was created by first collecting the fibers into a mat on a fluorine-doped tin oxide (FTO) plate. After the PVP shell was removed by soaking in ethanol, the nanofiber mat was then sandwiched in between an aluminum (Al) sputtered FTO substrate that was clamped together using binder clips. Because the mat was quite thick, the efficiency was quite low (8.7×10^{-8}). Bedford et al. [60] tried to build on this work by first depositing an electrospun mat and then depositing a P3HT:PCBM layer on top and reported an increase in efficiency of 25% over devices that did not include an electrospun mat.

Neither of the devices described above took full advantage of the electrospun fiber structure because the fibers were used in a mat configuration. By contrast, Nagata et al. have reported on the development and testing of electrospun polymer-fiber solar cells [61] using co-planar interdigitated electrodes of dissimilar materials (Figure 6) [62]. The device used an MEH-PPV:PCBM mixture and provided an efficiency of 3.08 $\times 10^{-7}$%. Although the reported efficiency was low, this device structure offers potential advantages when compared to more traditional structures. The use of interdigitated electrodes allows the utilization of very small fibers (diameters <1 μm) for improved exciton separation and charge collection. In addition, the use of an interdigitated structure results in multiple junctions (potentially thousands) so that the failure of one fiber has minimal impact on the overall device. Finally, because both of the electrodes are behind the active layer, they can be made from nontransparent materials, offering the designer a much wider range of electrode options.

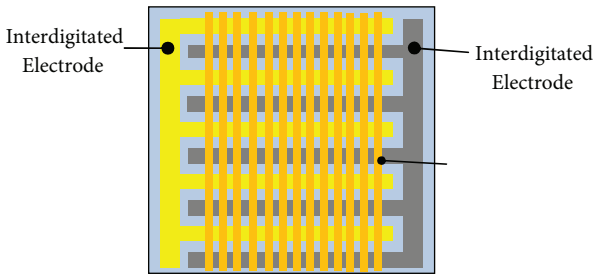

Figure 6. Electrospun polymer nanofiber solar cell on co-planar interdigitated electrodes.

4.3.2. Supramolecules

When the polymer in an organic photovoltaic absorbs light, excitons are generated. If the excitons are not within one diffusion length of a donor–acceptor interface, they will recombine before being separated. One idea that has been investigated to overcome this challenge is the synthesis of so-called supramolecules—molecules where the donor and acceptor are covalently attached within a single molecule. Unfortunately, these dyads [63–67] have not yielded high efficiencies. It has been surmised that the domain size within the molecule may be too small, resulting in recombination and poor charge carrier transport. As might be expected, in order to achieve both exciton diffusion and separation as well as charge transport, organic photovoltaics need an optimal domain size.

4.3.3. Solvents

One final way to impact the domain size is through the choice of solvents. In a comparison of the common solvents toluene and chlorobenzene with device based on PCBM and MDMO-PPV (poly[2-methoxy-53,7-dimethyloctyloxy)]-1,4-phenylenevinylene)), Hoppe et al [68] found that the choice of solvent had a significant

effect on the grain size. The toluene yielded grain sizes of 200–500 nm while the chlorobenzene yielded grain sizes of approximately 50 nm. This means that the grain size in the toluene-based devices is an order of magnitude larger than the exciton diffusion length while that in the chlorobenzene-based devices is much closer to the diffusion length. Therefore the devices made using chlorobenzene demonstrated a higher efficiency.

In addition to the actual solvent choice, the domain size also depends on the solvent evaporation time [69,70]. It has also been found that solvents with lower vapor pressure yield higher efficiencies–possibly due to better mixing of the polymer and the electron acceptor material [33]. Correspondingly, solvent evaporation times can impact the morphology and efficiency of the devices. Finally, the use of annealing can change the nanomorphology of the device and therefore impact the efficiency (increase or decrease) by changing the size of the domains. [68,71–74].

5. Conclusions

The efficiency of polymer-based organic solar cells has risen significantly over the past 10 years from approximately 3% [75] to nearly 11% [7]. While much of this increase can be attributed to the development of new polymers with increased quantum efficiency, the optimization of device structures has also played an important role. The incorporation of a variety of nanostructures in the design of organic polymer solar cells offers the possibility for even greater gains in efficiency.

References

[1] Huang, Y.; Pan, W.; Lai, Y.; Yang, T. T.; Chen, R.; Chirenjeevi, K.; Yu, P.; Meng, H.; Charlton, M.; Ehdp, E.; Iroorzhg, O.; Lrq, E. U. in *2013 IEEE 39th Photovoltaice Spec. Conf.*, IEEE, Tampa FL, 2013, pp. 1028–1030.

[2] Powell, D. M.; Winkler, M. T.; Goodrich, A.; Buonassisi, T. *IEEE J. Photovoltaics* **2013**, *3*, 662–668.

[3] Sun, S. S.; Sariciftci, N. S. *Organic Photovoltaics: Mechanisms, Materials, and Devices*, CRC Press: Boca Raton, FL, USA, 2005.

[4] Kapadia, R.; Yu, Z.; Wang, H.-H. H.; Zheng, M.; Battaglia, C.; Hettick, M.; Kiriya, D.; Takei, K.; Lobaccaro, P.; Beeman, J. W.; et al. *Sci. Rep.* **2013**, *3*, 2275.

[5] Kim, J. Y.; Lee, K.; Coates, N. E.; Moses, D.; Nguyen, T.-Q.; Dante, M.; Heeger, A. J. *Science* **2007**, *317*, 222–225.

[6] Reyes-Reyes, M.; Kim, K.; Carroll, D. L. *Appl. Phys. Lett.* **2005**, *87*, 083506.

[7] You, J.; Dou, L.; Yoshimura, K.; Kato, T.; Ohya, K.; Moriarty, T.; Emery, K.; Chen, C.-C.; Gao, J.; Li, G.; et al. *Nat. Commun.* **2013**, *4*, 1446.

[8] Gregg, B. A. *MRS Bull.* **2005**, *30*, 20–22.

[9] Huynh, W. U.; Peng, X.; Alivisatos, A. P. *Adv. Mater.* **1999**, *11*, 923–927.

[10] Fang, P. H.; Hirata, M.; Hirata, M. *Investigation of Organic Semiconductor for Photovoltaic Application*, Boston, 1972.

[11] Ghosh, A. K. *J. Appl. Phys.* **1973**, *44*, 2781.

[12] Lyons, L. E.; Newman, O. M. G. *Aust. J. Chem.* **1971**, *24*, 13–23.

[13] Mukherjee, T. K. **1970**, *377*, 3006–3014.

[14] Reucroft, P. J.; Kronick, P. L.; Hillman, E. E. *Research Directed toward the Study of Materials for Organic Solar Cells*, Philadelphia, 1968.

[15] Reucroft, P. J.; Kronick, P. L.; Hillman, E. E. *Mol. Cryst. Liq. Cryst.* **1969**, *6*, 247–254.

[16] Harima, Y.; Yamashita, K.; Suzuki, H. *Appl. Phys. Lett.* **1984**, *45*, 1144.

[17] Tang, C. W. *Appl. Phys. Lett.* **1986**, *48*, 183.

[18] Hoppe, H.; Sariciftci, N. S. *J. Mater. Res.* **2004**, *19*, 1924–1945.

[19] Fincher, C. J.; Peebles, D.; Heeger, A.; Druy, M.; Matsumura, Y.; MacDiarmid, A.; Shirakawa, H.; Ikeda, S. *Solid State* **1978**, *27*, 489–494.

[20] Sariciftci, N. S.; Braun, D.; Zhang, C.; Srdanov, V. I.; Heeger, A. J.; Stucky, G.; Wudl, F. *Appl. Phys. Lett.* **1993**, *62*, 585.

[21] Halls, J.; Walsh, C.; Greenham, N. *Nature* **1995**, *376*, 498–500.

[22] Yu, G.; Gao, J.; Hummelen, J. C.; Wudl, F.; Heeger, A. J. *Science (80-.).* **1995**, *270*, 1789–1791.

[23] Drees, M.; Premaratne, K.; Graupner, W.; Heflin, J. R.; Davis, R. M.; Marciu, D.; Miller, M. *Appl. Phys. Lett.* **2002**, *81*, 4607.

[24] Drees, M.; Davis, R.; Heflin, J. *Phys. Rev. B* **2004**, *69*, 165320.

[25] O'Regan, B.; Gratzel, M. *Nature* **1991**, *353*, 737–740.

[26] Grätzel, M. *J. Photochem. Photobiol. C Photochem. Rev.* **2003**, *4*, 145–153.

[27] Savenije, T. J.; Warman, J. M.; Goossens, A. **1998**, 148–153.

[28] Arango, A. C.; Carter, S. A.; Brock, P. J. *Appl. Phys. Lett.* **1999**, *74*, 1698.

[29] Fan, Q.; McQuillin, B.; Bradley, D. *Chem. Phys.* **2001**, *347*, 325–330.

[30] Grant, C. D.; Schwartzberg, A. M.; Smestad, G. P.; Kowalik, J.; Tolbert, L. M.; Zhang, J. Z. **2002**, *522*, 40–48.

[31] Breeze, A.; Schlesinger, Z.; Carter, S.; Brock, P. *Phys. Rev. B* **2001**, *64*, 125205.

[32] Ravirajan, P.; Haque, S. A.; Durrant, J. R.; Bradley, D. D. C.; Nelson, J. *Adv. Funct. Mater.* **2005**, *15*, 609–618.

[33] Kwong, C. Y.; Djurišić, a. B.; Chui, P. C.; Cheng, K. W.; Chan, W. K. *Chem. Phys. Lett.* **2004**, *384*, 372–375.

[34] Qiao, Q.; McLeskey, J. T. *Appl. Phys. Lett.* **2005**, *86*, 153501.

[35] Wright, M.; Uddin, A. *Sol. Energy Mater. Sol. Cells* **2012**, *107*, 87–111.

[36] Mor, G. K.; Shankar, K.; Paulose, M.; Varghese, O. K.; Grimes, C. A. *Appl. Phys. Lett.* **2007**, *91*, 152111.

[37] Peiro, A. M.; Ravirajan, P.; Govender, K.; Boyle, D. S.; O'Brien, P.; Bradley, D. D. C.; Nelson, J.; Durrant, J. R. *J. Mater. Chem.* **2006**, *16*, 2088.

[38] Baeten, L.; Conings, B.; Boyen, H.-G.; D'Haen, J.; Hardy, A.; D'Olieslaeger, M.; Manca, J. V; Van Bael, M. K. *Adv. Mater.* **2011**, *23*, 2802–2805.

[39] Yu, D.; Trad, T.; McLeskey, J. T.; Craciun, V.; Taylor, C. R. *Nanoscale Res. Lett.* **2010**, *5*, 1333–1339.

[40] Huynh, W. U.; Dittmer, J. J.; Alivisatos, A. P. *Science* **2002**, *295*, 2425–2427.

[41] Kymakis, E.; Amaratunga, G. a. J. *Appl. Phys. Lett.* **2002**, *80*, 112.

[42] Rud, J. A.; Lovell, L. S.; Senn, J. W.; Qiao, Q.; McLeskey, J. T. *J. Mater. Sci.* **2005**, *40*, 1455–1458.

[43] Dalal, V. *Electron Devices, IEEE Trans.* **1980**, 662–670.

[44] Peumans, P.; Bulovic, V.; Forrest, S. R. *Appl. Phys. Lett.* **2000**, *76*, 2650.

[45] Peumans, P.; Forrest, S. R. *Appl. Phys. Lett.* **2001**, *79*, 126.

[46] Yakimov, A.; Forrest, S. R. *Appl. Phys. Lett.* **2002**, *80*, 1667.

[47] Xue, J.; Uchida, S.; Rand, B. P.; Forrest, S. R. *Appl. Phys. Lett.* **2004**, *84*, 3013.

[48] Xue, J.; Uchida, S.; Rand, B. P.; Forrest, S. R. *Appl. Phys. Lett.* **2004**, *85*, 5757.

[49] Uchida, S.; Xue, J.; Rand, B. P.; Forrest, S. R. *Appl. Phys. Lett.* **2004**, *84*, 4218.

[50] Kawano, K.; Ito, N.; Nishimori, T.; Sakai, J. *Appl. Phys. Lett.* **2006**, *88*, 073514.

[51] Janssen, A. G. F.; Riedl, T.; Hamwi, S.; Johannes, H.-H.; Kowalsky, W. *Appl. Phys. Lett.* **2007**, *91*, 073519.

[52] Hadipour, A.; de Boer, B.; Blom, P. W. M. *J. Appl. Phys.* **2007**, *102*, 074506.

[53] Dennler, G.; Prall, H.-J.; Koeppe, R.; Egginger, M.; Autengruber, R.; Sariciftci, N. S. *Appl. Phys. Lett.* **2006**, *89*, 073502.

[54] Gilot, J.; Wienk, M. M.; Janssen, R. A. J. *Appl. Phys. Lett.* **2007**, *90*, 143512.

[55] Chen, C.-W.; Lu, Y.-J.; Wu, C.-C.; Wu, E. H.-E.; Chu, C.-W.; Yang, Y. *Appl. Phys. Lett.* **2005**, *87*, 241121.

[56] Peumans, P.; Uchida, S.; Forrest, S. R. *Nature* **2003**, *425*, 158–62.

[57] Zhou, Y.; Freitag, M.; Hone, J.; Staii, C.; Johnson, A. T.; Pinto, N. J.; MacDiarmid, A. G. *Appl. Phys. Lett.* **2003**, *83*, 3800.

[58] Babel, A.; Li, D.; Xia, Y.; Jenekhe, S. *Macromolecules* **2005**, 4705–4711.

[59] Sundarrajan, S.; Murugan, R.; Nair, A.; Ramakrishna, S. *Mater. Lett.* **2010**, *64*, 2369–2372.

[60] Bedford, N. M.; Dickerson, M. B.; Drummy, L. F.; Koerner, H.; Singh, K. M.; Vasudev, M. C.; Durstock, M. F.; Naik, R. R.; Steckl, A. J. *Adv. Energy Mater.* **2012**, *2*, 1136–1144.

[61] Nagata, S.; Atkinson, G.; Pestov, D.; Tepper, G. C.; McLeskey, J. T. *Adv. Mater.* **2013**, *975947*, 6.

[62] Nagata, S.; Atkinson, G. M.; Pestov, D.; Tepper, G. C.; McLeskey, J. T. *Sol. Energy Mater. Sol. Cells* **2011**, *95*, 1594–1597.

[63] Dhanabalan, A.; Knol, J. *Synth. Met.* **2001**, *119*, 519–522.

[64] Eckert, J.; Nicoud, J. *J. Am. Chem. Soc.* **2000**, *122*, 7467–7479.

[65] Antonietta Loi, M.; Denk, P.; Hoppe, H.; Neugebauer, H.; Winder, C.; Meissner, D.; Brabec, C.; Sariciftci, N. S.; Gouloumis, A.; Vázquez, P.; et al. *J. Mater. Chem.* **2003**, *13*, 700–704.

[66] Possamai, G.; Camaioni, N.; Ridolfi, G.; Franco, L.; Ruzzi, M.; Menna, E.; Casalbore-Miceli, G.; Fichera, A. M.; Scorrano, G.; Corvaja, C.; et al. *Synth. Met.* **2003**, *139*, 585–588.

[67] Roncali, J. *Adv. Energy Mater.* **2011**, *1*, 147–160.

[68] Hoppe, H.; Niggemann, M.; Winder, C.; Kraut, J.; Hiesgen, R.; Hinsch, A.; Meissner, D.; Sariciftci, N. S. *Adv. Funct. Mater.* **2004**, *14*, 1005–1011.

[69] Halls, J. J. M.; Arias, a. C.; MacKenzie, J. D.; Wu, W.; Inbasekaran, M.; Woo, E. P.; Friend, R. H. *Adv. Mater.* **2000**, *12*, 498–502.

[70] Strawhecker, K.; Kumar, S. *Macromolecules* **2001**, 4669–4672.

[71] Camaioni, N.; Ridolfi, G.; Casalbore-Miceli, G.; Possamai, G.; Maggini, M. *Adv. Mater.* **2002**, *14*, 1735–1738.

[72] Dittmer, J. J.; Lazzaroni, R.; Lecle, P.; Moretti, P.; Granstro, M.; Petritsch, K.; Marseglia, E. A.; Friend, R. H.; Bre, J. L.; Rost, H.; et al. **2000**, *61*, 53–61.

[73] Padinger, F.; Rittberger, R. S.; Sariciftci, N. S. *Adv. Funct. Mater.* **2003**, *13*, 85–88.

[74] Schmidt-Mende, L.; Fechtenkötter, A.; Müllen, K.; Moons, E.; Friend, R. H.; MacKenzie, J. D. *Science* **2001**, *293*, 1119–1122.

[75] Riedel, I.; Parisi, J.; Dyakonov, V.; Schilinsky, P.; Waldauf, C.; Brabec, C. J. in *Proc. SPIE - Int. Soc. Opt. Eng. Org. Photovoltaics V* (Eds.: Z.H. Kafafi, P.A. Lane), **2004**, pp. 82–89.